9940 *Inorg. Chem.* **2010**, *49*, 9940–9948
DOI: 10.1021/ic101210d

Inorganic Chemistry
Article

Efficient Fluorescent Sensors Based on 2,5-Diphenyl[1,3,4]oxadiazole: A Case of Specific Response to Zn(II) at Physiological pH

Gianluca Ambrosi,[†] Mauro Formica,[†] Vieri Fusi,*[,†] Luca Giorgi,[†] Eleonora Macedi,[†] Mauro Micheloni,*[,†] Paola Paoli,[‡] Roberto Pontellini,[†] and Patrizia Rossi[‡]

[†]*Institute of Chemical Sciences, University of Urbino, P.zza Rinascimento 6, I-61029 Urbino, Italy, and* [‡]*Department of Energy Engineering, University of Florence, Via S. Marta 3, I-50139, Firenze, Italy*

Received June 17, 2010

The coordination properties and photochemical responses of three fluorescent polyamine macrocycles, 9,12,15,24,25-pentaaza-26-oxatetracyclo[21.2.1.$0^{2,7}$.$0^{17,22}$]hexaicosa-2,4,6,17,19,21,23,25^{1}-octaene (**L1**), 9,12,15,18,27,28-hexaaza-29-oxatetracyclo[24.2.1.$0^{2,7}$.$0^{20,25}$]enneicosa-2,4,6,20,22,24,26,28^{1}-octaene (**L2**), and 9,12,15,18,21,30,31-heptaaza-32-oxatetracyclo[27.2.1.$0^{2,7}$.$0^{23,28}$]diatriconta-2,4,6,23,25,27,29,31^{1}-octaene (**L3**), toward Cu(II), Zn(II), Cd(II), and Pb(II) are reported. Each ligand contains the 2,5-diphenyl[1,3,4]oxadiazole (PPD) moiety inserted in a polyamine macrocycle skeleton. The stability constants were determined by means of potentiometric measurements in aqueous solution. **L1** forms mononuclear complexes only with Cu(II). **L2** and **L3** form stable mononuclear species with all of the metals, while **L3** is able to form dinuclear Cu(II) species. The fluorescence of all ligands was totally quenched by the presence of Cu(II). **L2** behaves as an OFF−ON sensor for Zn(II) under physiological conditions, even in the presence of interfering species such as Cd(II) and Pb(II). This ligand combines selective binding of Zn(II) with a highly specific fluorescent response to Zn(II) due to the chelating enhancement of fluorescence (CHEF) effect. The interaction of Zn(II), Cd(II), and Pb(II) with **L3** does not produce an appreciable enhancement of fluorescence at the same pH. The different behavior is attributed to the cavity size of the macrocycle and to the number of amine functions. **L2** possesses the best arrangement of these two characteristics, allowing a full participation of all of the amine functions in metal coordination, as shown by the crystal structures of [Cu**L2**(ClO_4)](ClO_4)·H_2O and [Zn**L2**Br]Br·H_2O species; this prevents the PET effect and supplies the higher CHEF effect. The interaction between **L2** and Zn(II) can also be observed with the naked eye as an intense sky blue emission.

Introduction

Among the trace elements involved in human metabolism, zinc is the most ubiquitous, and its physiological importance has long been recognized. More than 100 specific enzymes require zinc for their catalytic function.[1] Zinc participates in all major biochemical pathways and plays multiple roles in the perpetuation of genetic material, including transcription of DNA, translation of RNA, and ultimately cell division.[2] Zinc also affects both nonspecific and specific immune factors, such as the integrity of the epithelial barrier and the function of neutrophiles, monocytes, macrophages, and lymphocytes.[3] Since the 1990s, many health organizations have convened expert committees to develop estimates of human zinc requirements,[4] as several diseases can in fact be ascribed to deficiency[2,5] or overexposure[6] to this metal. It is not easy to determine the exact amount of zinc in living systems, and for this reason, the development of new non-invasive and fast systems to estimate the zinc level in humans is still an open field of research. In this context, the development of fluorescent chemosensors with high selectivity toward Zn(II) in aqueous solution represents an urgent and important challenge in analytical chemistry, because fluorescence is a fast, simple, and noninvasive analytical method

*To whom correspondence should be addressed. Tel./Fax: +39-0722-350032. E-mail: vieri.fusi@uniurb.it (V.F.).

(1) Cousins, R. I. *Present Knowledge in Nutrition*; Zeigler, E. E., Filer, L. J., Eds.; ILSI Press: Washington, DC, 1996.
(2) Van Wouwe, J. P. *Eur. J. Pediatr.* **1989**, *149*, 2.
(3) (a) Duchateau, J.; Delepesse, G.; Vrijens, R.; Collet, H. *Am. J. Med.* **1981**, *70*, 1001. (b) Prasad, A. S.; Meftah, S.; Abdallah, J.; Kaplan, J.; Brewer, G. J.; Bach, J. F.; Dardenne, M. *J. Clin. Invest.* **1988**, *82*, 1202.
(4) (a) *Trace elements in human health and nutrition*; WHO, FAO, IAEA; WHO: Geneva, 2002. (b) *Dietary reference intakes of vitamin A, vitamin K, arsenic, boron, chromium, copper, iodine, iron, manganese, molybdenum, nickel, silicon and zinc*; Food and Nutrition Board, IOM; National Academy Press: Washington, DC, 2002.
(5) (a) Ambidge, K. M. *Acta Pediatr. Scand. Suppl.* **1986**, *323*, 52. (b) Bhutta, Z. A.; Black, R. E.; Brown, K. H.; Meeks Gardner, J.; Gore, S.; Hidayat, A.; Khatun, F.; Martorell, R.; Ninh, N. X.; Penny, M .E.; Rosado, J. L.; Roy, S. K.; Ruel, M.; Sazawal, S.; Shankar, A. *J. Pediatr.* **1999**, *135*, 689. (c) Umeta, M; West, C. E.; Haidar, J.; Deurenberg, P.; Hautvast, J. G. A. J. *Lancet* **2000**, *355*, 2021. (d) Shankar, A. H.; Genton, B.; Baisor, M.; Paino, J.; Tamja, S.; Adiguma, T.; Wu, L.; Rare, L.; Bannon, D.; Tielsch, J. M.; West, K. P., Jr; Alpers, M. P. *Am. J. Trop. Med. Hyg.* **2000**, *62*, 663.
(6) (a) Fosmire, G. J. *Am. J. Clin. Nutr.* **1990**, *51*, 225. (b) Prasad, A. S.; Brewer, G. J.; Schoomaker, E. B.; Rabbani, P. *JAMA* **1978**, *240*, 2166. (c) Chandra, R. K. *JAMA* **1984**, *252*, 1443. (d) Yadrick, M. K.; Kenney, M. A.; Winterfeldt, E. A. *Am. J. Clin. Nutr.* **1989**, *49*, 145.

Published on Web 09/27/2010

Chart 1. The Ligands

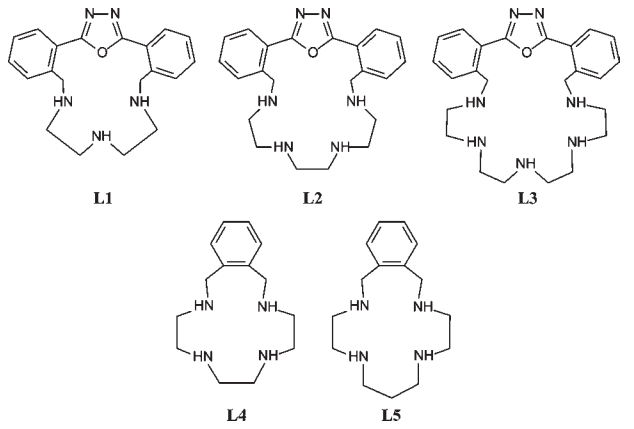

particularly suitable for *in vivo* applications. To reach this goal, research needs to be performed on the design and synthesis of ligands able to selectively bind a specific substrate and undergo concomitant changes in light absorption and/or emission properties.[7] In order to improve both selectivity and complex stability, preorganization is a fundamental requisite, and macrocycles and macropolycycles constitute the most important class of ligands useful for this aim.[8]

Recently, we reported the synthesis and spectroscopic properties of a new class of macrocyclic polyamines incorporating the 2,5-diphenyl[1,3,4]oxadiazole (PPD) fluorophore in their macrocyclic skeleton, constituted by 9,12,15,24,25-pentaaza-26-oxatetracyclo[21.2.1.$0^{2,7}$.$0^{17,22}$]hexaicosa-2,4,6,17,19,21,23,25^{1}-octaene (**L1**), 9,12,15,18,27,28-hexaaza-29-oxatetracyclo-[24.2.1.$0^{2,7}$.$0^{20,25}$]enneicosa-2,4,6,20,22,24,26,28^{1}-octaene (**L2**), and 9,12,15,18,21,30,31-heptaaza-32-oxatetracyclo-[27.2.1.$0^{2,7}$.$0^{23,28}$]diatriconta-2,4,6,23,25,27,29,31^{1}-octaene (**L3**) (Chart 1).[9] The insertion of PPD allowed a drastic improvement in the fluorescence quantum yield of these polyamine-based ligands over most of those already known, making these systems appealing for applications in the analysis of highly diluted analytes. To evaluate the use of these ligands as chemical sensors for metal ions in aqueous solution, and in particular for Zn(II), we explored the coordination and optical properties of **L1**−**L3** toward Cu(II), Zn(II), Cd(II), and Pb(II), paying particular attention to two crucial points: (i) the thermodynamic stability of the complexes and (ii) the photochemical response to coordination. In fact, not only does a powerful and selective sensor have to form stable adducts with the target analyte but the interaction also has to determine a strong change in optical properties. For fluorescent sensors, a drastic increase in emission upon guest interaction is desirable. Both the selectivity and efficiency of the response are closely dependent on the structure of the ligand, so in the present study, we monitored the effect of the macrocyclic size of **L1**−**L3** on their sensing behavior.

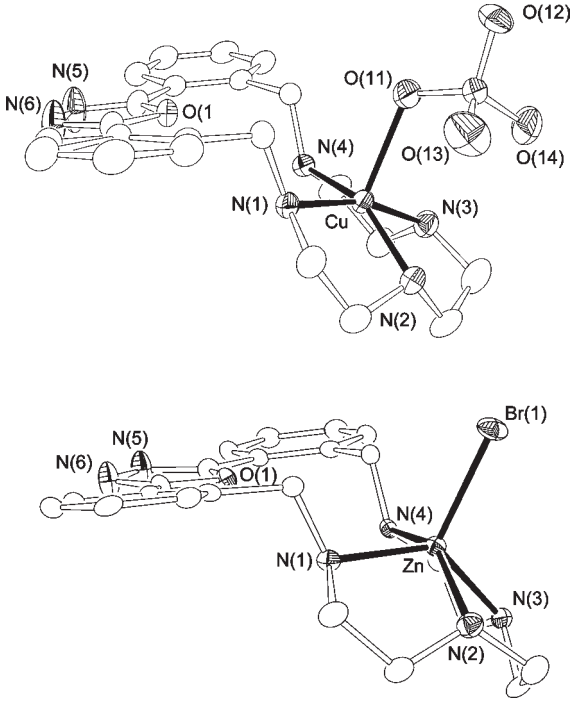

Figure 1. ORTEP3 views of the complex cations [Cu**L2**(ClO_4)]$^+$ of **1** (top) and [Zn**L2**Br]$^+$ of **2** (bottom). Hydrogen atoms have been omitted for the sake of clarity; thermal ellipsoids are drawn at 30% probability.

Results and Discussion

Solid State Studies. Both the crystal lattices of the Cu(II) and Zn(II) metal complexes [Cu**L2**(ClO_4)](ClO_4)·H_2O (**1**) and [Zn**L2**Br]Br·H_2O (**2**) are made up of the [M**L2**X]$^+$ complex cations (M = Cu(II), X = ClO_4^-; M = Zn(II), X = Br^-), the related counterions X^-, and crystallization water molecules (disordered over three positions in the case of the zinc sample). The overall shapes of the two metal complexes are almost identical (see Figure 1) as well as the coordination geometry around the metal cation. The metal complexes are penta-coordinated by the four nitrogen atoms provided by the polyamine moiety, with the counterion in the fifth position (see Figure 1). In the copper complex, an oxygen atom of the perchlorate ion occupies the axial position of a distorted sp (τ index 0.20),[10] while the bromide ion is the fifth donor atom of a distorted sp around the zinc ion, being τ = 0.30. In both cases, the metal cation is shifted (0.35 and 0.71 Å for copper and zinc, respectively) toward the apical donor with respect to the mean plane described by the four nitrogen atoms. The bond distances and angles defining the coordination sphere (Table S1, Supporting Information) are those expected for this kind of metal complex, as provided by a survey of homologous species deposited in the Cambridge Structural Database (V5.30, 2009).[11]

(7) (a) Lindoy, L. F. *The Chemistry of Macrocyclic Ligands Complexes*; Cambridge University Press: Cambridge, U. K., 1989. (b) Weber, E. *Crown Ethers and Analogs*; Patai, S., Rapport, A., Eds.; Wiley: New York, 1988. (c) Bradshaw, J. S. *Aza-crown Macrocycles*; Wiley: New York, 1993.

(8) (a) Czarnik, A. W. *Fluorescent Chemosensors for Ion and Molecule Recognition*; American Chemical Society: Washington, DC, 1993. (b) Bissel, R. A.; De Silva, A. P.; Gunaratne, H. Q. N.; Lynch, P. L. M.; Maguire, G. E.; McCoy, M. C. P.; Sandanayake, K. R. A. S. *Top. Curr. Chem.* **1993**, *168*, 223. (c) Bergonzi, R.; Fabbrizzi, L.; Licchelli, M.; Mangano, C. *Coord. Chem. Rev.* **1998**, *170*, 31. (d) De Silva, A. P.; Rupasinghe, R. A. D. D. *J. Chem. Soc., Chem. Commun.* **1996**, 1660. (e) Spichiger-Keller, U. E. *Chemical Sensors and Biosensors for Medical and Biological Applications*; Wiley-VCH: Weinheim, Germany, 1998. (f) Ellis, A. B.; Walt, D. R. *Chem. Rev.* **2000**, *100*, 2477 (Ellis, A. B.; Walt, D. R. Eds. Special issue on chemical sensors). (g) Aslin, E. V. *Tetrahedron* **2004**, *60*, 11055 (Aslin, E. V. Guest Ed. Special issue on synthetic receptors as sensors). (h) De Silva, A. P.; Tecilla, P. *J. Mater. Chem.* **2005**, *15*, 2617 (De Silva, A. P.; Tecilla, P. Guest Eds. Special issue on luminescent sensors).

(9) Ambrosi, G.; Formica, M.; Fusi, V.; Giorgi, L.; Macedi, E.; Micheloni, M.; Piersanti, G.; Pontellini, R. *Org. Biomol. Chem.* **2010**, *8*, 1471.

(10) Addison, A. W.; Rao, T. N.; Rijn, J.; Verschoor, G. C. *J. Chem. Soc., Dalton Trans.* **1984**, 1349.

(11) Allen, F. H. *Acta Crystallogr.* **2002**, *B58*, 380.

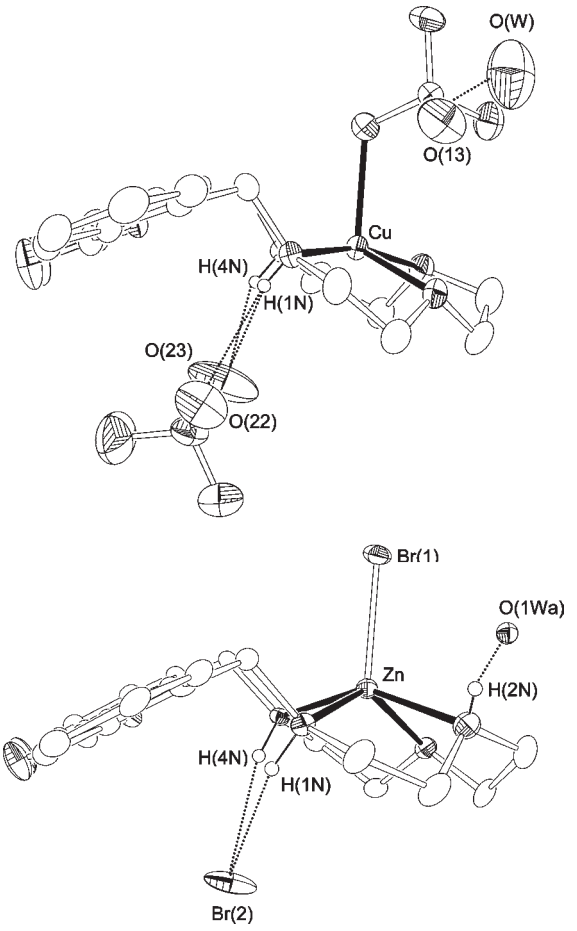

Figure 2. ORTEP3 views of the complex cations $[Cu\mathbf{L2}(ClO_4)]^+$ of **1** (top) and $[Zn\mathbf{L2}Br]^+$ of **2** (bottom) together with the counterions and the crystallization water molecules. Only the hydrogen atoms involved in the H bonds described in the text are shown; thermal ellipsoids are drawn at 30% probability.

The PPD macrocycle has a sort of chair shape, with the mean plane described by the three aromatic rings, which are in a plane, forming an angle of about 33° with that of the four nitrogen donors. The three ethylendiamine chains have the expected gauche conformation, with the central $HNCH_2CH_2NH$ unit differing in orientation. The counterion is located in the area defined by the aromatic system and the closest amine groups; it is held in place by a couple of hydrogen bonds of the X···HN type: Cl(2)O(23)···H(4N)N(4) (distance 2.21(3) Å, angle 158(3)°) and Cl(2)-O(23)···H(1N)N(1) (distance 2.54(3) Å, angle 151(3)°), in the copper complex; Br(2)···H(1N)N(1) (distance 2.45(4) Å, angle 165(3)°) and Br(2)···H(4N)N(4) (distance 2.61(4) Å, angle 164(4)°) in the zinc complex. In addition, the perchlorate counterion of the copper complex is held in place by a further H-bond interaction: Cl(2)O(22)···H(1)-N(1) (distance 2.46(3) Å, angle 149(3)°). Finally, in both the crystal lattices, the crystallization water molecule (disordered in the case of the zinc complex) occupies the same region with respect to the metal complex (see Figure 2). In the copper species, the molecule interacts with the oxygen atoms of the perchlorate anions (O(W)···O(13) 2.934(6) Å and O(W)···O(21) 2.987(6) Å, $x + 1$, y, z); in the zinc complex, O(1Wa) interacts with the hydrogen atom of an amine group (N(2)−H(2N)···O(1Wa) 2.34(5) Å, 138(5)°).

Table 1. Equilibrium Constants (log K) for the Metal Complex Equilibria of **L1**, Potentiometrically Determined in 0.15 mol dm^{-3} NaCl Aqueous Solution at 298.1 K

reaction	log K^a
$\mathbf{L1} + Cu^{2+} = Cu\mathbf{L1}^{2+}$	10.66(1)
$Cu\mathbf{L1}^{2+} + H^+ = CuH\mathbf{L1}^{3+}$	4.70(2)
$Cu\mathbf{L1}^{2+} + OH^- = Cu\mathbf{L1}(OH)^+$	6.46(2)

[a] Values in parentheses are the standard deviation on the last significant figure.

Table 2. Equilibrium Constants (log K) for the Metal Complex Equilibria of **L2**, Potentiometrically Determined in 0.15 mol dm^{-3} NaCl Aqueous Solution at 298.1 K

	log K^a			
reaction	Cu(II)	Zn(II)	Cd(II)	Pb(II)
$\mathbf{L2} + M^{2+} = M\mathbf{L2}^{2+}$	17.84(1)	10.41(1)	8.15(1)	8.04(1)
$M\mathbf{L2}^{2+} + H^+ = MH\mathbf{L2}^{3+}$	4.78(3)	5.90(2)	6.63(2)	6.65(3)
$M\mathbf{L2}^{2+} + OH^- = M\mathbf{L2}(OH)^+$	2.99(3)	5.29(2)	3.42(2)	3.41(3)
$M\mathbf{L2}(OH)^+ + OH^- = M\mathbf{L2}(OH)_2$		2.98(3)		

[a] Values in parentheses are the standard deviation on the last significant figure.

Table 3. Equilibrium Constants (log K) for the Metal Complex Equilibria of **L3**, Potentiometrically Determined in 0.15 mol dm^{-3} NaCl Aqueous Solution at 298.1 K

	log K^a			
reaction	Cu(II)	Zn(II)	Cd(II)	Pb(II)
$\mathbf{L3} + M^{2+} = M\mathbf{L3}^{2+}$	19.31(1)	11.50(1)	10.53(1)	9.34(1)
$M\mathbf{L3}^{2+} + H^+ = MH\mathbf{L3}^{3+}$	5.02(2)	6.47(3)	6.75(3)	7.57(2)
$MH\mathbf{L3}^{3+} + H^+ = MH_2\mathbf{L3}^{4+}$	3.49(2)			
$M\mathbf{L3}^{2+} + OH^- = M\mathbf{L3}(OH)^+$	3.73(3)	4.00(3)	3.69(3)	3.67(3)
$M\mathbf{L3}^{2+} + M^{2+} = M_2\mathbf{L3}^{4+}$	4.28(4)			
$M_2\mathbf{L3}^{4+} + OH^- = M_2\mathbf{L3}(OH)^{3+}$	7.69(4)			

[a] Values in parentheses are the standard deviation on the last significant figure.

In addition, in both crystal lattices, the complex cations interact with each other *via* NH···N hydrogen bonds.

Solution Studies. Potentiometric Studies. The coordination behavior of ligands **L1**, **L2**, and **L3** toward Cu(II), Zn(II), Cd(II), and Pb(II) was studied in aqueous 0.15 mol dm^{-3} NaCl at 298.1 K. The potentiometrically determined stability constants are reported in Tables 1−3, and the distribution diagrams of the species are reported in Figures 3 and 4 and S1 and S2 (Supporting Information).

L2 and **L3** form mononuclear complexes with all of the metal ions investigated, while **L1** binds only Cu(II) under these experimental conditions. **L3** is also able to form dinuclear species with Cu(II).

Mononuclear Complexes. The addition of Cu(II) to **L1** is rather low (log K = 10.66, see Table 1), and the value is in the range of the Cu(II) addition to ethylenediamines (log K = 10.44, 10.07, and 10.45 for ethylenediamine (EDA),[12] *N*,*N*′-dimethylethylenediamine (DMEDA),[13] and *N*,*N*′-diethylethylenediamine (DEEDA),[14] respectively). This suggests that **L1** most likely coordinates the metal ion with only two amine functions, leaving the third one unbound or weakly bound. In fact, the $[Cu\mathbf{L1}]^{2+}$ species is able to add a H^+ (log K = 4.70, Table 1) to form the protonated $[CuH\mathbf{L1}]^{3+}$ species, and this is in agreement with the previous statement because other tridentate

(12) Griesser, R.; Sigel, H. *Inorg. Chem.* **1971**, *10*, 229.
(13) Odani, A.; Yamauchi, O. *Inorg. Chim. Acta* **1984**, *93*, 13.
(14) Aihara, M.; Terasaki, T. *J. Inorg. Nucl. Chem.* **1981**, *43*, 323.

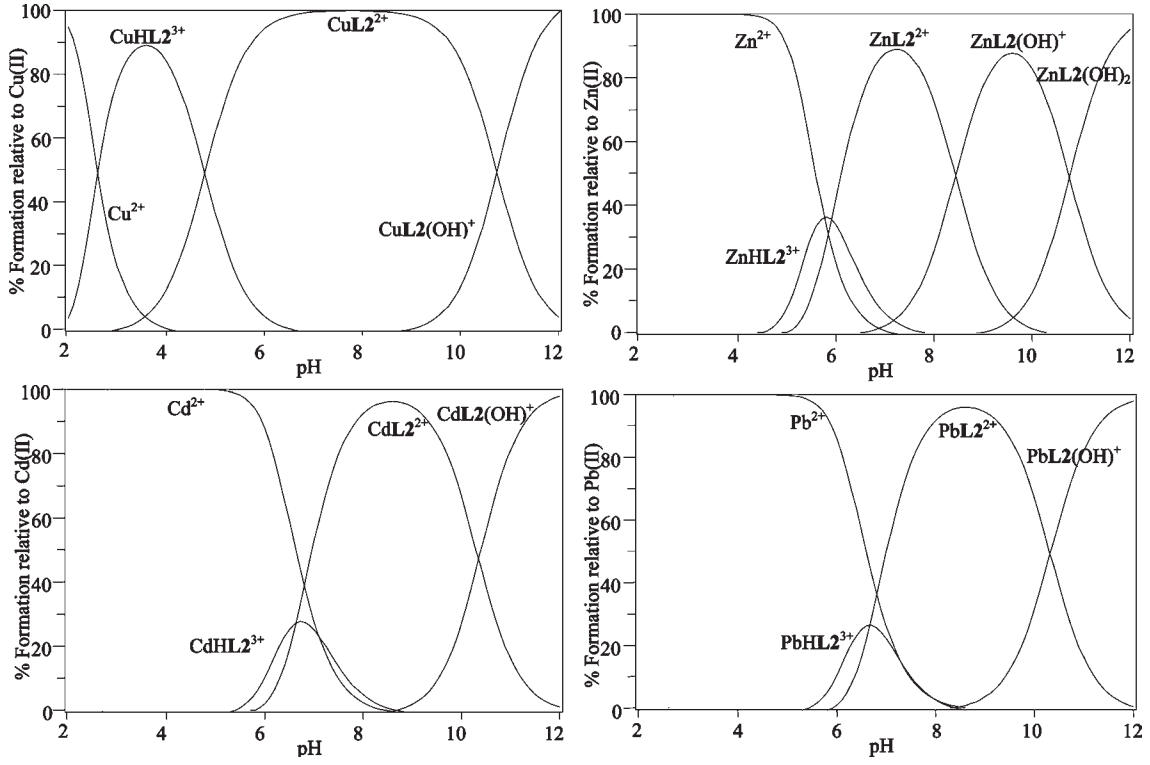

Figure 3. Distribution diagram for the **L2**/M(II) system in 0.15 M aqueous NaCl at 298.1 K ([**L2**] = 10^{-3} mol dm^{-3}; **L2**/M(II) = 1:1).

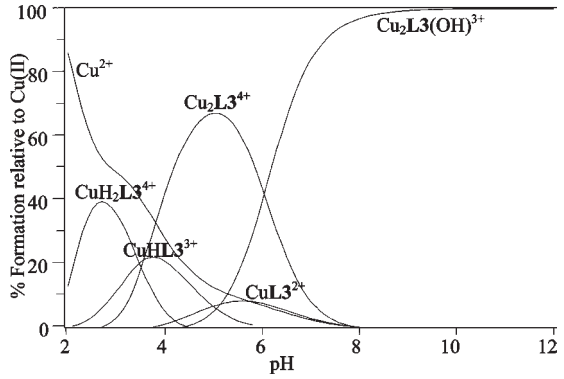

Figure 4. Distribution diagram for the **L3**/Cu(II) system in 0.15 M aqueous NaCl at 298.1 K ([**L3**] = 10^{-3} mol dm^{-3}; **L3**/Cu(II) = 1:2).

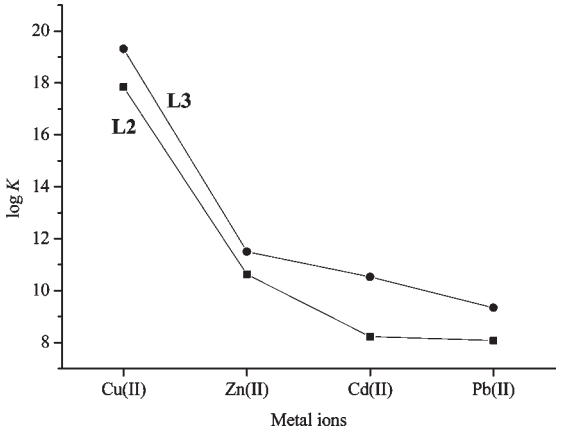

Figure 5. Trend of stability constants for [ML] species: M = Cu(II), Zn(II), Cd(II) and Pb(II); L = **L2** (■) and **L3** (●).

ligands showing all three amine functions strongly involved in the binding of Cu(II), such as [9]aneN$_3$ or diethylenetriamine (DETA), do not form protonated Cu(II) species even under strongly acidic conditions.[15] [Cu**L1**$_n$]$^{2+}$ (with n = 1, 2, or 3) species, which were found when ethylenediamine ligands coordinated the Cu(II),[16] were not detected in this case probably due to the steric hindrance of the PPD moiety. A water molecule coordinated to Cu(II) can be easily deprotonated, giving rise to the [Cu**L1**(OH)]$^{+}$ hydroxylated species with a high stability constant (log K = 6.46, for the addition of OH^{-} to [Cu**L1**]$^{2+}$).

In conclusion, **L1** probably binds M(II) with only two amine functions, since it is able to stabilize only Cu(II) under these experimental conditions. This can be ascribed to the small cavity size of **L1** and to the hindrance of PPD, which do not allow the involvement of all amine functions in the coordination of the metal ion.

On the contrary, both **L2** and **L3** form stable mononuclear [ML]$^{2+}$ species with all of the metal ions investigated (see Tables 2 and 3). The stability of the complexes follows the trend Cu(II) > Zn(II) > Cd(II) > Pb(II), with **L3** forming more stable [ML]$^{2+}$ species than **L2** for each metal (Figure 5). This behavior can be ascribed to the higher number of amine functions present in **L3** than in **L2** as well as to its greater flexibility.

One of the main questions related to the binding behavior of these ligands is whether the PPD heterocycle is involved or not in the coordination of metal ions. The crystal structures of **1** and **2**, reported in Figure 1, show that the PPD moiety is not involved in the coordination of

(15) Yang, R.; Zompa, L. J. *Inorg. Chem.* **1976**, *15*(7), 1499.
(16) Cotton, F. A.; Wilkinson, G.; Murillo, C. A.; Bochmann, M. *Advanced Inorganic Chemistry*, 6th ed.; J. Wiley and Sons, Inc., Wiley-Interscience: New York, 1999.

the metal ions in the solid state; in fact, this fragment is positioned far from the metal center, preventing a strong interaction with it. In addition, in the crystal structures reported in Figure 1, the two nitrogen atoms N(5) and N(6) of the oxadiazole heterocycle point toward the opposite side with respect to the polyamine macrocyclic ring. On this basis and considering the steric hindrance and the stiffness of the whole aromatic moiety, we can suppose that also in solution the PPD is not involved in the coordination of the metal and that the coordinating active framework is only provided by the polyamine chain; thus, the oxadiazole together with the two *ortho*-benzyl fragments can be considered only as a spacer. Seen in this light, the ligands would behave as polyaza *ortho*-cyclophanes, with both amine functions in the benzyl position involved in the stabilization of the metal ion.

For example, **L2** behaves like *ortho*-tetraazacyclophanes **L4** and **L5** (Chart 1) in binding Cu(II); **L4** and **L5** bind Cu(II) with the four amine functions, giving rise to stability constants similar to those of **L2** (log K_{CuL} = 17.84, 19.58,[17] and 17.73[17] for **L2**, **L4**, and **L5**, respectively), which provide further evidence for the lack of involvement of PPD in stabilizing these metal ions. In addition, the distance between the two benzyl nitrogens found in complex **1** (3.098(4) Å) is close to those published for $[Cu\mathbf{L5}Cl]^+$ (3.12 Å),[17] again supporting the previous statement. More generally, looking at the stability of the $[ML]^{2+}$ species, **L2** and **L3** suffer from the presence of the noncoordinating PPD moiety with respect to the other tetraaza macrocyclic ligands due to the formation of an energetically unfavorable large chelate ring (for example, the 12-membered chelate ring for **L2** shown in Figure 1).

^{1}H NMR experiments carried out on Zn(II), Cd(II), and Pb(II) complexes with **L2** and **L3** further supported the absence of interaction between PPD and the metal ion in solution; in fact, comparison of the complexes and the free ligands (see Figure S3, Supporting Information, for the Zn(II) complex) revealed that the aromatic part remains substantially unchanged while all aliphatic resonances undergo deep changes. Further evidence that PPD is not involved in metal coordination in solution will be reported in the spectrophotometric section.

All $[ML]^{2+}$ species of **L2** and **L3** can add at least one H^+ to give the protonated $[MHL]^{3+}$ species with proton affinity increasing from Cu(II) to Pb(II) complexes (Tables 2 and 3); for example, in the case of **L2**, the addition constant of H^+ to the $[M\mathbf{L2}]^{2+}$ species is log K = 4.78, 5.90, 6.63, and 6.65 for the Cu(II), Zn(II), Cd(II), and Pb(II) species, respectively. This is an opposite trend compared to the stability formation constants for related $[M\mathbf{L2}]^{2+}$ species, suggesting that all amine functions are involved in the coordination of the metal. In fact, considering this hypothesis, the protonation must break one M−N bond; thus this bond is weaker and the value of the protonation constant is higher .

However, taking into account that PPD is not involved in the stabilization of the metal ions and that **L3** exhibits only slightly greater stability than **L2** in the formation of the $[ML]^{2+}$ species, mainly for $[ZnL]^{2+}$, ($\Delta\log K_{ML}$ = 1.47, 1.09, 2.38, and 1.3 for Cu(II), Zn(II), Cd(II), and Pb(II), respectively), it is possible to suppose that the five amine functions of **L3** are not all strongly involved in the stabilization of the M(II) ions.

All of the $[ML]^{2+}$ species of **L2** and **L3** form stable monohydroxylated species with the $[ML(OH)]^+$ formula, with the exception of the $[Zn\mathbf{L2}]^{2+}$ species that is also able to form the $[Zn\mathbf{L2}(OH)_2]$ dihydroxylated species. These species are present in the alkaline range of pH (see Figure 3). The formation of such species highlights that both ligands do not fulfill the coordination requirement of the metal in the $[ML]^{2+}$ species, which thus behaves as a possible metallo-receptor for secondary ligands in addition to OH^-, as shown for **L2** by the crystal structures of **1** and **2**.

Dinuclear Complexes. L3 is the only ligand able to form dinuclear species, but only with Cu(II) among the several metal ions investigated; this can be ascribed to its larger cavity size and higher number of donor nitrogen atoms with respect to **L1** and **L2**, as well as to its high affinity toward Cu(II). The value for the addition of the second Cu(II) to the $[Cu\mathbf{L3}]^{2+}$ species to form the $[Cu_2\mathbf{L3}]^{4+}$ dinuclear species is not highly favorable (log K = 4.28, Table 3). In fact, considering the number of binding functions of **L3** and the full involvement of the five amine functions in the stabilization of the first Cu(II), the insertion of the second Cu(II) must occur with a rearrangement of the Cu(II)−N bonds in the complex (breaking of old Cu(II)−N and formation of new Cu(II)−N bonds); in any case, both Cu(II)'s are coordinated by **L3** with a low coordination number. For this latter reason, the $[Cu_2\mathbf{L3}]^{4+}$ species, which shows two highly unsaturated Cu(II) ions, easily adds secondary ligands, as was found in the case of the OH^- anion. The favorable addition of the hydroxide to the $[Cu_2\mathbf{L3}]^{4+}$ species is underlined by the value of 7.69 logarithmic units for the formation constant of the reaction $[Cu_2\mathbf{L3}]^{4+} + OH^- = [Cu_2\mathbf{L3}(OH)]^{3+}$ (Table 3), which is in the range of a hydroxide anion bridging two Cu(II) cations.[18] The distribution diagram of the species (Figure 4) shows that for the ratio **L3**/Cu(II) = 1:2, $[Cu_2\mathbf{L3}(OH)]^{3+}$ is the main species present in solution at pH > 6.5.

UV−vis Studies. Spectrophotometric and spectrofluorimetric studies were carried out in order to evaluate the use of these ligands as sensors for metal ions and the role of the PPD moiety in the coordination of metal ions. In a previous paper,[9] we established that the emission properties of **L1**−**L3** are PET-regulated by electron transfer from the lone pairs of the amine functions to the HOMO of the excited fluorophore;[8a] as a consequence, the coordination of a suitable metal ion into the macrocyclic moiety should affect the emission intensity by preventing the PET. A preliminary screening was carried out by slow titration of buffered solutions of the ligands with the metal ions (Cu(II) for **L1** and Cu(II), Zn(II), Cd(II), and Pb(II) for **L2** and **L3**), choosing, for each ligand−metal system, the pH at which the $[ML]^{2+}$ species are predominant in solution (see distribution of the species

(17) Chadim, M.; Diaz, P.; Garcia-España, E.; Hodacova, J.; Junk, P. C.; Latorre, J.; Llinares, J. M.; Soriano, C.; Zavada, J. *New J. Chem.* **2003**, *27*, 1132.

(18) (a) Dapporto, P.; Formica, M.; Fusi, V.; Micheloni, M.; Paoli, P.; Pontellini, R.; Rossi, P. *Inorg. Chem.* **2000**, *39*, 4663. (b) Dapporto, P.; Formica, M.; Fusi, V.; Giorgi, L.; Micheloni, M.; Paoli, P.; Pontellini, R.; Rossi, P. *Inorg. Chem.* **2001**, *40*, 6186.

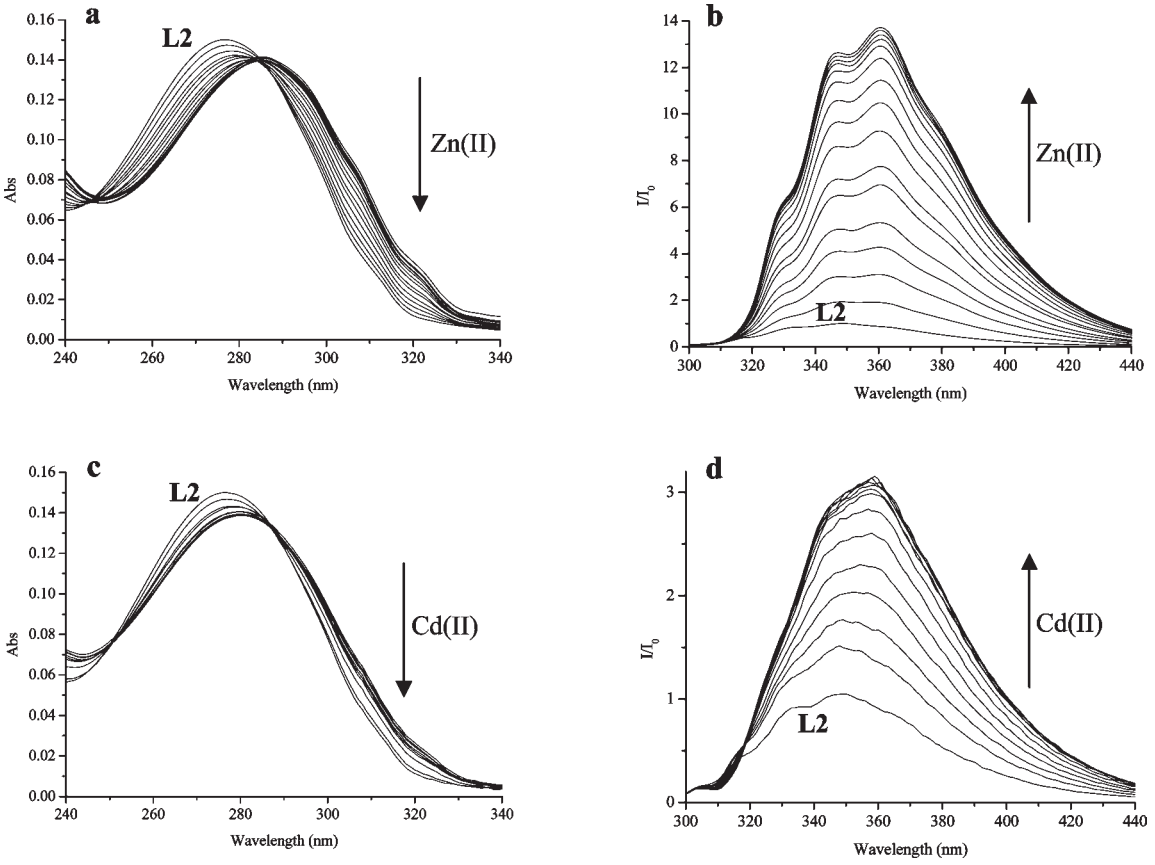

Figure 6. Variation of the absorption (a) and emission (b) spectra of **L2** by adding $Zn(ClO_4)_2$: pH = 7.4 (HEPES 0.05 mol dm^{-3} adjusted with NaOH 0.2 mol dm^{-3}), [**L2**] = 10^{-5} mol dm^{-3}, [Zn^{2+}] = from 0 to 10^{-5} mol dm^{-3}, λ_{ex} = 285 nm. Variation of the absorption (c) and emission (d) spectra of **L2** by adding $Cd(ClO_4)_2$: pH = 8.6 (TAPS 0.05 mol dm^{-3} adjusted with NaOH 0.2 mol dm^{-3}), [**L2**] = 10^{-5} mol dm^{-3}, [Cd^{2+}] = from 0 to 10^{-5} mol dm^{-3}, λ_{ex} = 290 nm.

in Figures 3 and S1 and S2, Supporting Information). As expected, all emissions of the ligands were quenched upon Cu(II) complexation due to the paramagnetic-metal effect that promotes the ISC from the S_1 state to T_1.[19] With regard to the other metal ions, an increase in the emission intensity was observed by adding Zn(II) and Cd(II) to **L2** and by adding only Zn(II) to **L3**. Figure 6 reports the absorption and emission spectra obtained by titration of a buffered aqueous solution of **L2** with Zn(II) and Cd(II) perchlorate; the figures for Cu(II) and Pb(II) titration are reported in the Supporting Information (Figure S4). The absorption spectra of the **L2**/Zn(II) system at pH = 7.4, where the $[ZnL2]^{2+}$ species prevails in solution, show that the interaction of the metal ion with **L2** produces a red shift in the absorption band from 276 nm for the free ligand to 286 nm for the complex (Figure 6a). The emission band, measured under the same conditions by excitation at the isosbestic point (285 nm), undergoes a similar red shift upon Zn(II) addition (from 349 nm for **L2** to 361 nm for the complex, see Figure 6b); this behavior, similar to those observed in the previous protonation studies, is determined by the stabilization of the PPD excited state in the complex due to the presence of positive charged species in the macrocycle.[9] Moreover, this shift is too small to be ascribed to a direct interaction of the fluorophore with the metal ion, once again indicating that the PPD does not participate in the metal ion coordination. The complexation gives rise to a 14-fold enhancement of the fluorescence signal (CHEF) with respect to free **L2** (Figure 6b) due to the partial inhibition of the PET effect caused by the engagement of the macrocycle amine lone pairs in the metal coordination.[8] An analogous effect, but of lower magnitude, was observed for the **L2**/Cd(II) system at pH = 8.6, where the $[CdL2]^{2+}$ species is prevalent in solution. In this case, the coordination of the metal ion gives rise to a red shift of 4 nm in the absorption band (from 276 to 280 nm, see Figure 6c) and of 9 nm in the emission band (from 349 to 358 nm, λ_{ex} = 290 nm), with a CHEF quantifiable at 3-fold enhancement with respect to the emission of the free ligand (see Figure 6d). No significant optical effects were observed for the **L2**/Pb(II) system at pH = 8.4, where the $[PbL2]^{2+}$ species prevails in solution (Figure S4c,d, Supporting Information).

Analogous experiments were performed for the **L3**/M(II) systems in aqueous solution. In this case, as outlined above, only the interaction with Cu(II) and Zn(II) yields spectroscopic changes (Figure S5, Supporting Information) despite the fact that this ligand forms more stable complexes with the other metal ions (see Potentiometric Studies section). The fluorescence emission increases only 4-fold upon Zn(II) complexation (Figure S5d, Supporting Information), which means that in this case the metal ion does not inhibit the PET as it does in the case of **L2**. Due to the larger cavity size of **L3**, the nitrogen lone pairs are probably not as engaged in the bond with Zn(II) as

(19) (a) Gilbert, A.; Baggott, J. *Essentials of Molecular Photochemistry*, Blackwell: Oxford, U. K., 1991. (b) Turro, N. J. *Modern Molecular Photochemistry*; University Science Books: Mill Valley, CA, 1991.

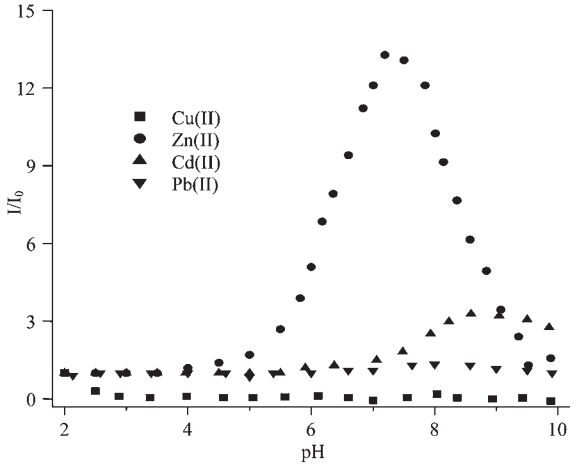

Figure 7. Relative emission intensity (I/I_0) as a function of pH for **L2** in aqueous solution in the presence of 1 equiv of each metal ion ([**L2**] = 10^{-5} mol dm^{-3}; I and I_0 are the emission intensity of **L2** in the presence and absence of the metal ion, respectively).

they are in **L2**, allowing a residual PET that can justify the reduced CHEF.[20]

In light of these studies, it follows that **L3** forms more stable complexes than **L2**, but the latter offers the best photochemical response upon metal complexation. This would be due to a better matching between the number of donor sites and the size of the cavity. In fact, the number of donor sites and the stability of the complexes are higher, but an excessive number of lone pairs together with a too large cavity makes it more difficult to control the PET by metal complexation.

The photochemical properties of **L2**/M(II) systems as a function of pH were also monitored. Figure 7 reports the differences between the emission behavior of the ligand in the absence and presence of the metal ion, expressed as relative emission intensity I/I_0 where I is the emission intensity in the presence of M(II) and I_0 is the intensity in the absence of M(II). An in-depth analysis of the Zn(II) and Cd(II) systems revealed that only the $[M\mathbf{L2}]^{2+}$ species behaves differently from the free **L2**. For example, merging the fluorescence data related to the **L2**/Zn(II) system with the corresponding distribution diagram reported in Figure 3, the relative emission intensity (I/I_0) increases from pH = 5, where $[Zn\mathbf{L2}]^{2+}$ appears, and drops from pH = 7.5 to pH = 10, where this species disappears in solution; in other words, only the $[Zn\mathbf{L2}]^{2+}$ species is significantly more fluorescent than the free **L2**. This behavior can be explained when taking into account that the $[Zn\mathbf{L2}]^{2+}$ species prevails in the pH range where the free ligand is in the diprotonated form, with low fluorescence[9] giving a high I/I_0 ratio. On the contrary, the protonated $[ZnH\mathbf{L2}]^{3+}$, present in solution from pH = 4 to pH = 8, is fluorescent but has a quantum yield similar to that of the protonated $H_3\mathbf{L2}^{3+}$ ligand that, in the absence of Zn(II), prevails in approximately the same pH range. The same occurs at pH > 10 where hydroxylated $[Zn\mathbf{L2}(OH)]^{+}$ and $[Zn\mathbf{L2}(OH)_2]$ species are prevalent in solution; these are not emitting species due to the elongation of the M−N ligand caused by the OH^- complexation,

(20) Bencini, A.; Bernardo, M. A.; Bianchi, A.; Fusi, V.; Giorgi, C.; Pina, F.; Valtancoli, B. *Eur. J. Inorg. Chem.* **1999**, 1911.

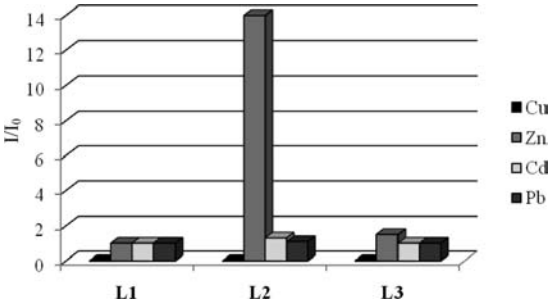

Figure 8. Relative emission intensity (I/I_0) upon addition of the metal ion (1 equiv) to the ligands in water at pH = 7.4 (HEPES 0.05 mol dm^{-3} adjusted with NaOH 0.2 mol dm^{-3}; I and I_0 are the emission intensity of the ligand in the presence and absence of the metal ion, respectively).

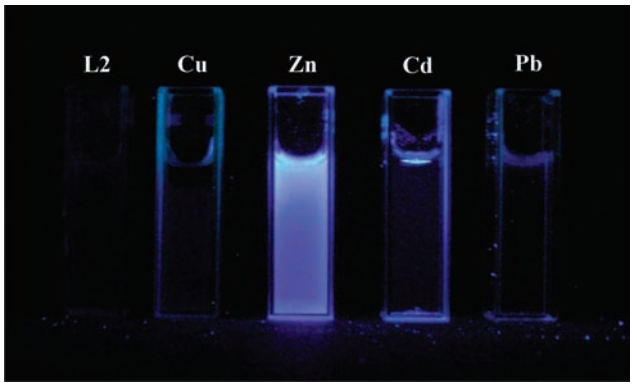

Figure 9. Photo of **L2** samples irradiated by a UV lamp upon the addition of 1 equiv of Cu(II), Zn(II), Cd(II), and Pb(II) perchlorates ([**L2**] = 10^{-5} mol dm^{-3} in 0.05 mol dm^{-3} aqueous HEPES, pH = 7.4, LP Hg lamp λ_{ex} = 254 nm).

which restores the PET, thus behaving similarly to the free **L2** in this range. It should be underlined, as depicted in Figure 7, that **L2** acts as a specific sensor for Zn(II) in a narrow range of pH centered at pH = 7.4, where **L2** is highly sensitive only to the presence of Zn(II), increasing its emission 14-fold upon the metal coordination, while it is not influenced by the presence of Cd(II) and Pb(II) at this pH (Figure 7).

At pH = 7.4, **L3** drastically decreases its sensitivity toward Zn(II), as expected upon examination of the relative distribution diagram reported in Figure S2, Supporting Information.

Thus, on the basis of these observations, we can conclude that only ligand **L2** possesses both the optimal cavity size and number of nitrogen donor groups to behave as a selective sensor for Zn(II) at physiological pH. The histogram shown in Figure 8 reports the changes in emission intensity of all three ligands upon interaction with the metal ion tested at pH = 7.4; it is clear that **L2** can be used as an OFF−ON fluorescence sensor specific for Zn(II), given that the increase of fluorescence emission is so high that it can be seen even with the naked eye (Figure 9).

Concluding Remarks

This paper describes the coordination behavior toward Cu(II), Zn(II), Cd(II), and Pb(II) of a series of fluorescent sensors, namely, **L1**, **L2**, and **L3**. Each sensor contains the fluorophore 2,5-diphenyl[1,3,4]oxadiazole (PPD) inserted in polyaza macrocycle fragments of different cavity sizes and

numbers of secondary amine functions. All the ligands are highly soluble in water in the examined range of pH 2−12, and their photochemical properties are PET regulated, as the ligands are highly fluorescent in strongly acidic media and quenched beginning from about pH = 8. **L1** forms mononuclear complexes only with Cu(II). **L2** and **L3** form stable mononuclear complexes with all four metals, and **L3** is also able to form dinuclear Cu(II) species. The fluorescence of all the ligands is totally quenched by the presence of Cu(II). **L2** behaves as an efficient OFF−ON sensor for Zn(II) at physiological pH (pH = 7.4), even in the presence of interfering species such as Cd(II) and Pb(II), because the ligand combines the selective binding of Zn(II) over Cd(II) and Pb(II) with the highly specific fluorescent response to the presence of Zn(II) due to the chelating enhancement of fluorescence (CHEF) effect; the emitting species is $[ZnL2]^{2+}$. On the contrary, the interaction of Zn(II), Cd(II), and Pb(II) with **L3** does not produce significant increases of fluorescence at the same pH. The different behavior of the ligands is due to the different size of the macrocyclic cavity together with the number of amine functions. In fact, **L3** forms more stable $[ML]^{2+}$ species than **L2** for each metal due to the higher number of amine functions present in this ligand with respect to **L2**, but the difference between the respective stability constants is rather small, ranging from $\Delta\log K_{ML} = 1.09-2.38$. This means that in the complexed species of **L3** the five nitrogens are not strongly involved in the coordination, giving a residual PET; thus, this system remains quenched in the presence of coordinated metal ions. On the contrary, **L2** offers the best matching between cavity size and number of amine functions, allowing the full participation of all of the donor atoms in the metal coordination and thus preventing the PET and giving the higher CHEF effect with Zn(II). In these ligands the regulation of the fluorescence is PET mediated, and the switching-on is due to the full involvement of the amine lone pairs in the metal complexation. In fact, no direct interaction between the fluorophore PPD and the metal ion was detected. The wide emission band of the $[ZnL2]^{+}$ complex centered at 361 nm reaches the visible region, allowing the interaction to be detected even with the naked eye as an intense sky blue emission upon excitation with an inexpensive LP Hg lamp (254 nm).

Experimental Section

General Methods. ***Caution!*** *Perchlorate salts of organic compounds are potentially explosive; these compounds must be prepared and handled with care!*

UV absorption spectra were recorded at 298 K on a Varian Cary-100 spectrophotometer equipped with a temperature control unit. Fluorescence emission spectra were recorded at 298 K on a Varian Cary-Eclypse spectrofluorimeter, and the spectra are uncorrected. All reagents and solvents used were of analytical grade.

EMF Measurements. Equilibrium constants for protonation and complexation reactions of the ligands were determined by pH-metric measurements in 0.15 mol dm^{-3} NaCl at 298.1 ± 0.1 K, using the fully automatic equipment that has already been described;[21a] EMF data were acquired with the PASAT computer program.[21b] The combined glass electrode was calibrated as a hydrogen concentration probe by titrating known amounts of HCl with CO_2-free NaOH solutions and determining the equivalent point using Gran's method,[21c,d] which gives the standard potential E° and the ionic product of water (pK_w = 13.83(1) at 298.1 K in 0.15 mol dm^{-3} NaCl, $K_w = [H^+][OH^-]$). At least three potentiometric titrations were performed for each system in the pH range 2−12, and all titrations were treated either as single sets or as separate entities, for each system. No significant variations were found in the values of the determined constants. The HYPERQUAD computer program was used to process the potentiometric data.[21e]

Synthesis. Ligands 9,12,15,24,25-pentaaza-26-oxatetracyclo-[21.2.1.$0^{2,7}$.$0^{17,22}$]hexaicosa-2,4,6,17,19,21,23,25[1]-octaene (**L1**), 9,12,15,18,27,28-hexaaza-29-oxatetracyclo[24.2.1.$0^{2,7}$.$0^{20,25}$]-enneicosa-2,4,6,20,22,24,26,28[1]-octaene (**L2**), and 9,12,15,18,21,30,31-heptaaza-32-oxatetracyclo[27.2.1.$0^{2,7}$.$0^{23,28}$]diatriconta-2,4,6,23,-25,27,29,31[1]-octaene (**L3**) were prepared as reported.[9]

[CuL2(ClO_4)](ClO_4)·H_2O (1). A sample of $Cu(ClO_4)_2\cdot 6H_2O$ (37 mg, 0.1 mmol) in water (15 cm^3) was added to an aqueous solution (15 cm^3) containing **L2**·4HBr (72 mg, 0.1 mmol). The pH of the resulting solution was adjusted to 7 with 0.1 M NaOH and saturated with solid $NaClO_4$. After a few minutes, **1** precipitated as a microcrystalline blue-green solid (58 mg, 84%). Anal. Calcd for $C_{22}H_{30}Cl_2CuN_6O_{10}$: C, 39.27; H, 4.49; N, 12.49. Found: C, 39.4; H, 4.7; N, 12.3. Crystals suitable for X-ray analysis were obtained by slow evaporation of an aqueous solution containing **1**.

[ZnL2Br]Br·H_2O (2). A sample of $Zn(ClO_4)_2\cdot 6H_2O$ (37 mg, 0.1 mmol) in water (15 cm^3) was added to an aqueous solution (15 cm^3) containing **L2**·4HBr (72 mg, 0.1 mmol). The pH of the resulting solution was adjusted to 7 with 0.1 M NaOH and saturated with solid KBr. After a few minutes, **2** precipitated as a microcrystalline white solid (49 mg, 77%). Anal. calcd for $C_{22}H_{30}Br_2N_6O_2Zn$: C, 41.57; H, 4.76; N, 13.22. Found: C, 41.8; H, 5.0; N, 13.1. Crystals suitable for X-ray analysis were obtained by slow evaporation of an aqueous solution containing **2**.

X-Ray Structures. Intensity data for compounds **1** and **2** were collected on an Oxford Diffraction Excalibur diffractometer using Mo Kα radiation (λ = 0.71073 Å). For both compounds, the diffractometer was equipped with a cryocooling device, which has been used to set the temperature at 150 K. Data collections were performed with the program CrysAlis CCD.[22] Data reduction for both structures was carried out with the program CrysAlis RED.[23] For both structures, the absorption correction was applied using the ABSPACK[24] program.

The structures were solved using the SIR-97 package[25] and subsequently refined on the F^2 values using the full-matrix least-squares program SHELXL-97.[26]

Concerning compound **1**, all of the non-hydrogen atoms were refined anisotropically. The hydrogen atoms bonded to the nitrogen atoms of the ligand were found in the Fourier syntheses and their positions refined; all of the other hydrogen atoms of the ligand were set in calculated positions and refined with isotropic thermal parameters depending on the atom to which they were bound. The hydrogen atoms of the water molecule were not introduced in the refinement.

All of the non-hydrogen atoms, with the exception of the oxygen one of the disordered water molecule, in **2** were refined

(21) (a) Dapporto, P.; Fusi, V.; Micheloni, M.; Palma, P.; Paoli, P.; Pontellini, R. *Inorg. Chim. Acta* **1998**, *168*, 275. (b) Fontanelli, M.; Micheloni; M. *1st Spanish-Italian Congress: Thermodynamics of Metal Complexes*, Peñiscola, Spain, June 3−6, 1990; University of Valencia: Valencia, Spain, 1990. (c) Gran, G. *Analyst* **1952**, *77*, 661. (d) Rossotti, F. J.; Rossotti, H. *J. Chem. Educ.* **1965**, *42*, 375. (e) Gans, P.; Sabatini, A.; Vacca, A. *Talanta* **1996**, *43*, 1739.

(22) *CrysAlis CCD*, version 1.171.pre23_10 beta (release 21.06.2004 CrysAlis171.NET); Oxford Diffraction Ltd.: Oxfordshire, U. K., 2004.

(23) *CrysAlis RED*, Version 1.171.pre23_10 beta (release 21.06.2004 CrysAlis171.NET); Oxford Diffraction Ltd.: Oxfordshire, U. K., 2004.

(24) *ABSPACK in CrysAlis RED*, Version 1.171.29.2 (release 20−01−2006 CrysAlis171 .NET); Oxford Diffraction Ltd.: Oxfordshire , U. K., 2006.

(25) Altomare, A.; Cascarano, G. L.; Giacovazzo, C.; Guagliardi, A.; Burla, M. C.; Polidori, G.; Camalli, M. *J. Appl. Crystallogr.* **1999**, *32*, 115.

(26) Sheldrick, G. M. *SHELX 97*; University of Göttingen: Göttingen, Germany, 1997.

Table 4. Crystallographic Data and Refinement Parameters for Compounds **1** and **2**

	1	**2**
empirical formula	[Cu**L2**(ClO_4)](ClO_4)·H_2O	[Zn**L2**Br]Br·H_2O
fw	672.96	635.71
temperature (K)	150	150
wavelength (Å)	0.71073	0.71073
cryst syst, space group	monoclinic, $P2_1/n$	monoclinic, $P2_1/n$
unit cell dimensions (Å, deg)	a = 9.3390(2)	a = 8.4756(3)
	b = 15.2362(5), β = 96.276(3)	b = 14.5446(4), β = 99.038(3)
	c = 19.3439(5)	c = 20.2935(7)
volume (Å^3)	2735.96(13)	2470.6(1)
Z, D_c (mg/cm^3)	4, 1.634	4, 1.709
μ (mm^{-1})	1.060	4.260
cryst shape, color	prism, blue-green	prism, white
cryst size (mm)	0.50 × 0.45 × 0.30	0.45 × 0.40 × 0.38
final R indices [$I > 2\sigma(I)$]	R1 = 0.0552, wR2 = 0.1265	R1 = 0.0453, wR2 = 0.1073
R indices (all data)	R1 = 0.1501, wR2 = 0.1438	R1 = 0.0826, wR2 = 0.1138
GOF	0.792	0.918

anisotropically. The hydrogen atoms bonded to the nitrogen atoms of the ligand were found in the Fourier map and refined isotropically. All of the other hydrogen atoms were set in calculated positions and refined with isotropic thermal parameters depending on the atom to which they were bound. The disorder of the water molecule was modeled using three oxygen atoms with an occupancy factor of 0.33. The hydrogen atoms of the water molecule were not introduced in the refinement.

Geometrical calculations were performed using PARST97,[27] and molecular plots were produced using the ORTEP3 program.[28]

Crystallographic data and refinement parameters are reported in Table 4.

CCDC 775506 and 775507 contain the supplementary crystallographic data for this paper. These data can be obtained free of charge from the Cambridge Crystallographic Data Centre via www.ccdc.cam.ac.uk/data_request/cif.

Acknowledgment. The authors thank the Italian Ministero dell'Istruzione dell'Università e della Ricerca (MIUR), PRIN2007 for financial support. CRIST (Centro di Crystallografia Strutturale) University of Florence, where the X-ray measurements were performed, and Dr. Samuele Ciattini are gratefully acknowledged.

Supporting Information Available: Table of selected bond distances and angles for complexes **1** and **2**, distribution diagrams for Cu(II)/**L1** and M(II)/**L3** systems, ^{1}H NMR spectra for the Zn(II)/**L2** system, additional UV−vis and fluorescence spectra, and crystallographic data in CIF format. This material is available free of charge via the Internet at http://pubs.acs.org.

(27) Nardelli, M. *J. Appl. Crystallogr.* **1995**, *28*, 659.
(28) Farrugia, L. J. *J. Appl. Crystallogr.* **1997**, *30*, 565.